Apparent Ionic Charges and Vibrational Eigenmodes of $BaTiO_3$ and Other Perovskites*

J. D. AXE
IBM Watson Research Center, Yorktown Heights, New York
(Received 2 December 1966)

The polarization associated with the vibrations of a complex lattice can be discussed by assigning apparent charges to the individual ions. These apparent charges can be calculated for a lattice of electrically polarizable ions by a consideration of the local dipole fields if polarization due to short-range forces is neglected, and such calculations are made for several cubic perovskites. Using these calculations as criteria for reasonable values of apparent charges results in the severe restriction of the range of the displacements permissible for the polar vibrational modes compatible with the experimentally observed mode dipole strengths. The apparent ionic charges and polar eigenmodes of $SrTiO_3$, $BaTiO_3$, $KTaO_3$, and $KCoF_3$ are discussed in this manner. For $BaTiO_3$, the magnitude of the spontaneous polarization is correctly predicted, and the displacements predicted for the very low-frequency mode in the cubic phase are closely similar to those which occur at the cubic-tetragonal phase transformation.

I. INTRODUCTION

WITHIN recent years, the understanding of displacive ferroelectric materials, as exemplified by $BaTiO_3$, has been deepened as a result of the consideration of the onset of the ferroelectric instability from the standpoint of lattice dynamics.[1–5] In essence, it is now established that displacive ferroelectrics are characterized above their Curie temperature T_c by one or more transverse optical-phonon branches whose frequency in the long-wavelength limit tends to zero approximately as $(T-T_c)^{1/2}$. Cowley's fitting of a shell model to the inelastic neutron-scattering data for $SrTiO_3$ gives the most complete confirmation, but it is not entirely obvious how these results are to be generalized to other perovskites of interest. Since the vibrations of importance for the ferroelectric phenomenon are those of long wavelength, it is possible to learn a great deal by studying the interaction of these modes with electromagnetic radiation. In particular, knowledge of the dielectric response of a lattice as a function of frequency, as can be obtained from analysis of infrared reflectivity measurements, gives the long-wavelength normal-mode frequencies and associated polarizations in a very direct way.[3,4,6,7]

Previous discussions of the dynamics of the perovskite lattice (with one exception[7]) have not made use of the dipole strength of the vibrational modes. The vibrational displacements of the ions of a lattice can be related to the associated dipole moments through a set of apparent ionic charges. This paper is a consideration of the apparent charges and polar eigenmodes of several cubic perovskites and how they may be deduced from infrared dielectric dispersion data. These quantities, deduced entirely from the dynamical properties of the cubic phase, can be used to make predictions concerning the displacements and spontaneous polarization of possible ferroelectric phases. In the case of $BaTiO_3$, these predictions are largely verified.

In the following section the equations determining the long-wavelength lattice dynamics of a complex lattice are reviewed in order to properly introduce the concept of apparent charge. This is followed by an extension of Slater's[8] discussion of the Lorentz correction in the perovskite structure to include a consideration of such dynamical quantities as apparent charges and sublattice coupling constants. This is done to provide a basis both for subsequent approximations and the understanding of results which they provide.

II. PHENOMENOLOGICAL THEORY

In order to properly define the lattice dynamical quantities of interest, it is necessary to discuss a general phenomenological theory of dielectric dispersion in complex lattices. Such a treatment has been discussed by Born and Huang[9] and others.[7,10] Following the more condensed matrix notation of Cochran and Cowley,[10] it is supposed that the energy density within a dielectric can be specified by the most general quadratic function of two quantities; the electric field vector, $\mathbf{E}\exp i(\mathbf{q}\cdot\mathbf{r}-\omega t)$, and $\mathbf{U}\exp i(\mathbf{q}\cdot\mathbf{r}-\omega t)$, a $3n$-dimensional vector representing the displacements of the n atoms within a unit cell. In the long-wavelength limit ($\mathbf{q}\to 0$), the optical vibrations of the lattice are deter-

* Partially supported by Army Research Office under Contract No. DA-31-124ARO-D-205.

[1] P. W. Anderson, in *Fizika Dielectrikov*, edited by G. I. Skanovi (Akad. Nauk SSSR, Moskow, 1960).
[2] W. Cochran, Advan. Phys. **9**, 387 (1960).
[3] A. S. Barker and M. Tinkham, Phys. Rev. **125**, 1527 (1960).
[4] W. G. Spitzer, R. C. Miller, D. A. Kleinman, and L. E. Howard, Phys. Rev. **126**, 1710 (1960); R. C. Miller and W. G. Spitzer, *ibid.* **129**, 94 (1963).
[5] R. A. Cowley, Phys. Rev. **134**, A981 (1964).
[6] J. T. Last, Phys. Rev. **105**, 1740 (1957).
[7] T. Kurosawa, J. Phys. Soc. Japan **16**, 1298 (1961). The discussion of $BaTiO_3$ contained here is in some aspects simliar to the present work, but was handicapped by the lack of dielectric dispersion measurements.
[8] J. C. Slater, Phys. Rev. **78**, 748 (1950).
[9] M. Born and K. Huang, *Dynamical Theory of Crystal Lattices* (Oxford University Press, New York, 1964).
[10] W. Cochran and R. A. Cowley, J. Phys. Chem. Solids **23**, 447 (1961).

mined by three equations,

$$\omega^2\mathbf{mU}=\mathbf{MU}-\mathbf{QE}, \tag{1}$$

$$\mathbf{P}=(1/v)\mathbf{Q}^{\dagger}\mathbf{U}+\chi\mathbf{E}, \tag{2}$$

$$\mathbf{E}=-(4\pi/q^2)(\mathbf{q}\cdot\mathbf{P})\mathbf{q}+\mathbf{E}_0. \tag{3}$$

$\mathbf{m}$ is a diagonal matrix specifying the mass of each of the n atoms and $\mathbf{M}$ is the $3n\times3n$ dynamical matrix representing the force constants pertaining to displacement of the n sublattices relative to one another. $\mathbf{P}\exp i(\mathbf{q}\cdot\mathbf{r}-\omega t)$ is the dielectric polarization vector and v is the volume of the unit cell. The derivatives of the macroscopic polarization with respect to the displacement vectors make up the $3n\times3$ matrix of apparent charge, $\mathbf{Q}$ ($\mathbf{Q}^{\dagger}$ is its transpose). χ is by definition the electronic dielectric susceptibility tensor. The macroscopic electric field $\mathbf{E}$ is written as a sum of an externally applied field $\mathbf{E}_0$ and that due to the polarization charge density, $-\mathrm{div}\,\mathbf{P}$.

For cubic crystals, the above equations factor into three identical sets referring to vector components along crystallographic axes, and only one set, say the αth, need be discussed. Furthermore, in the absence of applied external fields, the eigenmodes are purely longitudinal or transverse, the latter having no associated electric field [see Eq. (3)], but capable of interacting in first order with electromagnetic radiation. The transverse eigensolutions are simply

$$\Omega_j^2\mathbf{mu}_{\alpha j}=\mathbf{Mu}_{\alpha j} \qquad (j=1,\,n), \tag{4}$$

where the eigenvectors can be orthonormalized according to $\mathbf{u}_{\alpha j'}{}^{+}\mathbf{mu}_{\alpha j}=N\delta_{jj'}$, N being any convenient normalization constant. One of the eigenfrequencies, $\Omega_1=0$, represents the $q=0$ limit of an acoustic branch. The remaining $n-1$ Ω_j are termed dispersion frequencies, as it is possible to express the dielectric response as

$$\epsilon_{\alpha\alpha}(\omega)-\epsilon_{\alpha\alpha}{}^{\infty}=\sum_j \Delta\epsilon_j\Omega_j^2/(\Omega_j^2-\omega^2), \tag{5a}$$

$$\Delta\epsilon_j=(4\pi/Nv\Omega_j^2)|\mathcal{P}_{\alpha j}|^2, \tag{5b}$$

$$\epsilon_{\alpha\alpha}{}^{\infty}=1+4\pi\chi_{\alpha\alpha}{}^{\infty}, \tag{6}$$

where $(\mathcal{P}_{\alpha j})$ is (to within a normalization constant) the dipole moment associated with the jth transverse eigenmode,

$$\mathcal{P}_{\alpha j}=\sum Q_{\kappa,\alpha}u_{\kappa,\alpha j}. \tag{7}$$

(It is useful to introduce double indices to differentiate between spatial coordinates α, $\beta=x$, y, z and the ions κ, κ' within the unit cell. In subsequent sections reference will always be to one of the three identical Cartesian coordinates of a cubic system and the subscript α will be suppressed.) A sketch of the perovskite unit cell is shown in Fig. 1. For ions occupying the A or B sites, symmetry considerations dictate that the components of the apparent charges along the principal axes be identical. An X ion has an apparent charge $Q_{X\parallel}$ for displacements along the $B-X$ axis which is in general different than $Q_{X\perp}$ for displacements perpendicular to the $B-X$ axis. There are thus four apparent charge parameters for the perovskite lattice.

III. APPARENT CHARGES IN THE DIPOLE LOCAL-FIELD APPROXIMATION

If the ions were unpolarizable charged entities, their apparent charges as defined would be isotropic and identical with their net static charges Z_i. In fact the ions have substantial electronic polarizabilities which must produce and interact with local electric fields at the lattice sites. In order to develop some insight into the magnitude of the apparent charges for the perovskite lattice it is helpful to consider the approximation in which the electronic dipole moments of the ions are taken to be proportional to the local electric field at the ion site produced by the dipole moments of the remaining ions. The expressions for χ^{∞}, $\mathbf{Q}$, and $\mathbf{M}$ in this approximation can be derived from a discussion of the dynamics of a lattice of polarizable ions given by Born and Huang,[9] and for a cubic lattice are as follows[11]:

$$(\epsilon^{\infty}-1)/4\pi=\chi^{\infty}=(1/v)\sum_{\kappa,\kappa'}\Gamma_{\kappa,\kappa'}, \tag{8}$$

$$Q_{\kappa}=Z_{\kappa}\sum_{\kappa}(\mathbf{1}-\mathbf{C\Gamma})_{\kappa,\kappa'}, \tag{9}$$

$$M_{\kappa,\kappa'}=[\mathbf{R}+\mathbf{Z}(\mathbf{C}-\mathbf{C\Gamma C})\mathbf{Z}]_{\kappa,\kappa'}. \tag{10}$$

The dynamical matrix is divided into a short-range part $\mathbf{R}$ and a remainder expressing the electrostatic forces between dipoles and point charges. $\mathbf{Z}$ is a diagonal matrix representing the static charges of the ions, and

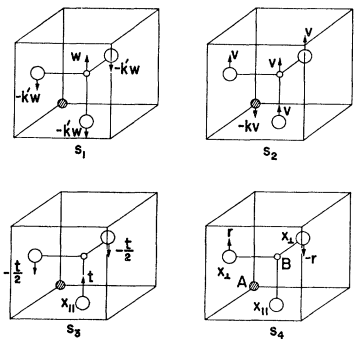

FIG. 1. Symmetry coordinates for long-wavelength vibrations of the perovskite lattice. Coordinates S_1, S_2, and S_3 transform as Γ_{15} and are optically active, whereas S_4 transforming as Γ_{25} is not. $k'=(m_B/3m_x)$ and $k=(m_B+3m_x)/m_A$. The relative displacements u_{kj} are indicated. They must be normalized according to $\Sigma m_\kappa u^2{}_{kj}=N$.

[11] It is also instructive to derive Eqs. (8)–(11) from a more general model which includes short-range polarization effects. They can be obtained from the shell model in the form used by Cochran (Ref. 2) by letting the shell charges Y_κ, the core charges X_κ, and the shell-core coupling k_κ all increase without limit, but in such a way as to keep the net ion charge $Z_\kappa=Y_\kappa+X_\kappa$, and electronic polarizability, $\alpha_\kappa=Y_\kappa{}^2/k_\kappa$, finite. Thus there exists an electronic moment $p_\kappa=Y_\kappa W_\kappa$ even though the relative displacement of the shell from the core W_κ goes to zero.

the elements of the Coulomb matrix **C** are closely related to the Lorentz corrections for the local fields.[2]

$$\mathbf{C}=(1/v)\begin{pmatrix} C_{11} & r & r-p & r+\frac{1}{2}p & r+\frac{1}{2}p \\ r & C_{22} & r+q & r-\frac{1}{2}q & r-\frac{1}{2}q \\ r-p & r+q & C_{33} & r+\frac{1}{2}p & r+\frac{1}{2}p \\ r+\frac{1}{2}p & r-\frac{1}{2}q & r+\frac{1}{2}p & C_{44} & r-p \\ r+\frac{1}{2}p & r-\frac{1}{2}q & r+\frac{1}{2}p & r-p & C_{55} \end{pmatrix}, \tag{11}$$

where $r=-4\pi/3=-4.189$, $q=-30.080$, and $p=-8.668$. The diagonal elements of **C** are given from the condition for translational invariance of Eq. (10), which requires $\sum_{\kappa'} Z_{\kappa'}C_{\kappa\kappa'}=0$. The matrix $\mathbf{\Gamma}$ which relates the macroscopic field to the dipole moments at the lattice sites is given by

$$(\mathbf{\Gamma}^{-1})_{\kappa\kappa'}=[C_{\kappa,\kappa'}+\delta_{\kappa,\kappa'}(\alpha_\kappa^{-1}+C_0-C_{\kappa,\kappa})], \tag{12}$$

where α_κ is the electronic polarizability of the κth ion, and $C_0=-4\pi/3v$.

This procedure of accounting for the electronic susceptibility by a local electric field acting upon an electronic polarizability of the ions is not however rigorously justifiable, although it is in common use. The recent successes of the shell model[5,12] have demonstrated the additional necessity of recognizing a dipole-moment contribution due to deformation of the ions by short-range repulsive interactions with their neighbors. Cochran has shown that the shell model is only compatible with the local-field model if the outer electron shells are coupled so tightly to their cores that the displacements of both the shells and the cores go to zero at high frequencies.[11] From a more empirical point of view, Szigeti[13] has shown by analysis of data for many ionic diatomic cubic crystals (e.g., NaCl) that short-range polarization effects cause the charge parameters Z_i to differ by 10~30% from the formal ionic charges. The local-field expressions (8)–(11) might therefore be expected to yield qualitative rather than quantitatively accurate information.

In order to utilize Eqs. (8)–(12), it is only necessary to introduce electronic polarizabilities appropriate for the constituent ions. These equations were evaluated for four compounds: $BaTiO_3$, $SiTiO_3$, $KTaO_3$, and $KCoF_3$. The fitting procedure adopted consisted of selecting, where possible, generally accepted values of electronic ion polarizabilities and adjusting by trial and error one of the polarizabilities (usually that of the anion) by a small amount to obtain the observed value of ϵ^∞ via Eq. (8). In the case of $KTaO_3$, the oxygen polarizability was taken as that for $SrTiO_3$ and the Ta^{5+} polarizability was adjusted.[14] The results for the apparent charges are given in Table I for the four materials. There are three principle predictions which can be deduced from a study of the results of this model.

TABLE I. The apparent charges of several cubic perovskites in the dipole local-field approximation.

	$BaTiO_3$	$SrTiO_3$	$KTaO_3$	$KCoF_3$
ϵ_∞	5.31[a]	5.20[b]	4.35[c]	2.07[d]
v (Å^3)	64.4	59.6	63.6	64.0
α_A (Å^3)	2.33[a]	1.60[e]	1.32	1.33
Q_A/Z_A	2.36	2.27	2.01	1.34
α_B (Å^3)	0.186[a]	0.186	0.00	0.34
Q_B/Z_B	2.69	3.25	2.45	1.43
α_X (Å^3)	2.17[a]	2.21	2.21	0.79
$Q_{X\|\|}/Z_{X\|\|}$	6.42	7.80	7.46	2.27
$Q_{X\perp}/Z_{X\perp}$	0.66	0.48	−0.16	0.96

[a] W. N. Lawless, Phys. Rev. **138**, A1751 (1965). The polarizabilities are corrected for electronic dispersion.
[b] M. Cardona, Phys. Rev. **140**, A651 (1965).
[c] R. C. Miller and W. G. Spitzer, Phys. Rev. **129**, 94 (1963).
[d] J. D. Axe and G. D. Pettit, following paper, Phys. Rev. **157**, 43 (1967).
[e] Tessman, Kahn, and Shockley, Phys. Rev. **92**, 890 (1953). The values of α_X were adjusted slightly to give observed ϵ_∞. For $KTaO_3$, α_0 found for $SrTiO_3$ and $\alpha_{Ta}=0$ were found to give the measured ϵ_∞.

(1) The long-range $B-X_{||}$ sublattice coupling is greatly enhanced. The interaction is attractive and thus in opposition to the repulsive short-range contribution. In a diagonally cubic lattice (each atom having tetrahedral or higher point symmetry), all the atoms have the same local field and the long-range portion of the dynamical matrix becomes simply $L_{ij}=-(4\pi e^2/9v)(\epsilon_\infty+2)Z_iZ_j$. For $BaTiO_3$ this amounts to $-10.2\ Z_{Ti}Z_O(e^2/v)$ for the Ti–$O_{||}$ sublattice, whereas the value using the correct perovskite internal field is $-115.9\ Z_{Ti}Z_O(e^2/v)$. None of the other sublattice couplings are so dramatically enhanced relative to the diagonally cubic case.

(2) The apparent charges of the anions are quite anisotropic, $Q_{X||}$ being enhanced relative to a diagonally cubic lattice, $Q_{X\perp}$ being greatly reduced.

(3) Although the preceding statements are true for all four lattices, they are much less pronounced for the fluoride. The local-field enhancement of the long-range $B-X_{||}$ coupling is reduced to $-59.2\ Z_{Co}Z_F(e^2/v)$. This reflects chiefly the fact that the fluoride ion is roughly half as polarizable as is the oxygen ion.

It may be pointed out that the local-dipole field treatment just presented can be viewed as a self-consistent extension of Slater's[8] discussion of the perovskite local field to include those parameters characterizing the lattice dynamical behavior. Through consideration

[12] R. A. Cowley, W. Cochran, A. D. B. Woods, and B. N. Brockhouse, Phys. Rev. **131**, 1030 (1963).
[13] B. Szigeti, Proc. Roy. Soc. (London), **A204**, 51 (1950).

[14] In order to evaluate the diagonal elements of the Coulomb matrix, the following simple assumption was made concerning the ratio of the static charges; $Z_A:Z_B:Z_X=1:2:-1:-1$. There is considerable evidence (discussed later) that this may be in error by 25% or so for $BaTiO_3$. An error much larger than this would be necessary to change the qualitative conclusions of the calculation however.

of the form of the expression for the high-frequency polarization, Slater was able to correctly identify the critical importance of the unusually favorable Lorentz factors existing for the perovskite structure. Specifically, he showed that in the case of $BaTiO_3$ it is only necessary to augment the electronic polarizability of the Ti ion in Eq. (8) by a fractionally small amount to produce a ferroelectric singularity in the susceptibility ($\chi \to \infty$), and that this additional ionic polarizability implied physically realistic ionic charges and displacements. One advantage of the lattice-dynamic approach afforded by Eqs. (1)–(3) is that the ionic contribution to the polarization is introduced in an integral and consistent manner, thereby avoiding the *ad hoc* introduction of ionic polarizabilities,[15] instead focusing attention on the concept of the apparent charge. Equation (9) allows the apparent charges to be estimated for a model consistent with Slater's treatment of the high-frequency polarization.

IV. ANALYSIS OF DISPERSION DATA

The aim of this section is to establish the form of the normal vibrations $\mathbf{u}_{\alpha j}$ and to assign apparent charges to the individual ions in accordance with the measured strength of the infrared resonances and with Eq. (7). The apparent charges obtained in the preceding section serve to define a range of reasonable values for the apparent charges obtained in this more empirical way.

It is convenient to discuss the normal vibrations of the perovskite lattice in terms of a complete set of coordinates constructed to form bases for irreducible representations of the group O_h, thereby factoring the eigenvalue problem to the maximum extent made possible by symmetry.[16] One such possible set is shown in Fig. 1. There is but a single possible mode of Γ_{25} symmetry, so that the normal mode of this symmetry is $\mathbf{u}_4=\mathbf{S}_4$. No unique set of symmetry coordinates exists for the Γ_{15} modes and the eigenvectors will in general consist of linear combinations of the three symmetry coordinates shown.

To proceed with this analysis, the Γ_{15} mode of highest frequency, Ω_3, will be assumed to have the eigenvector $\mathbf{u}_3=\mathbf{S}_3$. This is a good approximation to the result of Cowley's detailed fitting of a shell model to the $SrTiO_3$ phonon-dispersion data.[5] In their more approximate discussion, Joseph and Silverman[17] also arrive at a description of the highest frequency mode quite similar to this approximation for both $SrTiO_3$ and $KTaO_3$. Physically, such a solution is favored by light anion masses and strong anion-anion coupling, the latter factor probably being the more important. Strong anion-anion coupling comes about because the long-range forces between two anion sublattices are repulsive and are thus augmented rather than diminished by short-range repulsion. Slater[18] has called attention to the important contribution the close approach of negative ions makes in determining the size and energy of ionic lattices. The above considerations are a natural extension of these arguments.

Since by hypothesis $\mathbf{u}_3=\mathbf{S}_3$, the unitary transformation relating the Γ_{15} symmetry coordinates $\mathbf{S}_i$ to the eigenvectors $\mathbf{u}_i$ become simply

$$\begin{pmatrix}\mathbf{u}_1\\ \mathbf{u}_2\\ \mathbf{u}_3\end{pmatrix}=\begin{pmatrix}\cos\xi & -\sin\xi & 0\\ \sin\xi & \cos\xi & 0\\ 0 & 0 & 1\end{pmatrix}\begin{pmatrix}\mathbf{S}_1\\ \mathbf{S}_2\\ \mathbf{S}_3\end{pmatrix},$$

so that the entire eigenvector problem is reduced to the specification of the single parameter ξ. By choosing $\mathbf{S}_1$ and $\mathbf{S}_2$ as given in Fig. 1, the eigenvectors once they are found can be simply discussed in relation to these rather idealized limiting behaviors. However more information is required to establish the criteria for a best-fitting value of ξ corresponding to a given physical situation.

The additional information which is readily available from the infrared measurements is the mode strength $\Delta\epsilon_j$. A summary of the experimentally determined dispersion frequencies and mode strengths for several perovskites are shown in Table II. Using Eq. (5b) to relate the mode strengths to the mode polarization vectors $|\mathcal{P}_{\alpha j}|^2$ and the $\mathbf{u}_j(\xi)$ just introduced, it is possible to arrive at a set of apparent charges $Q(\xi)$ consistent with the observed mode strengths and the assumed con-

TABLE II. The infrared dispersion frequencies and dipole strengths of several cubic perovskites.

	$BaTiO_3$[a]	$SrTiO_3$[b]	$KTaO_3$[c]	$KCoF_3$[d]
ω_1 (cm^{-1})	42	87	85	139
$\Delta\epsilon_1$	1250	299	209	1.96
ω_2 (cm^{-1})	182	178	199	225
$\Delta\epsilon_2$	2.2	3.6	5.0	2.21
ω_3 (cm^{-1})	500	546	549	417
$\Delta\epsilon_3$	0.8	1.9	2.4	0.83

[a] J. M. Ballantyne, Phys. Rev. **136**, A429 (1964); A. S. Barker, Jr., Phys. Rev. **145**, A391 (1966).

[b] A. S. Barker and M. Tinkham, Phys. Rev. **125**, 1527 (1960); W. G. Spitzer, R. C. Miller, D. A. Kleinman, and L. E. Howard, *ibid.* **126**, 1710 (1960); R. C. Miller, and W. G. Spitzer, *ibid.* **129**, 94 (1963).

[c] W. G. Spitzer, R. C. Miller, D. A. Kleinman, and L. E. Howard, Phys. Rev. **126**, 1710 (1960); R. C. Miller and W. G. Spitzer, *ibid.*, **129**, 94 (1963).

[d] J. D. Axe and G. D. Pettit, following paper, Phys. Rev. **157**, 435 (1967).

[15] The concept of an ionic polarizability is imprecisely defined and the source of much confusion. Cochran (Ref. 2) concludes that on the basis of the shell model the concept can only be legitimized for diagonally cubic crystals, in which case the local field at every atom is identical.

[16] E. B. Wilson, Jr., J. C. Decius, and P. C. Cross, *Molecular Vibrations* (McGraw-Hill Book Company, Inc., New York, 1955), p. 113.

[17] R. I. Joseph and B. D. Silverman, J. Phys. Chem. Solids **24**, 1349 (1963); **25**, 1125 (1964).

[18] J. C. Slater, *Quantum Theory of Molecules and Solids* (McGraw-Hill Book Company, Inc., New York, 1965), p. 108.

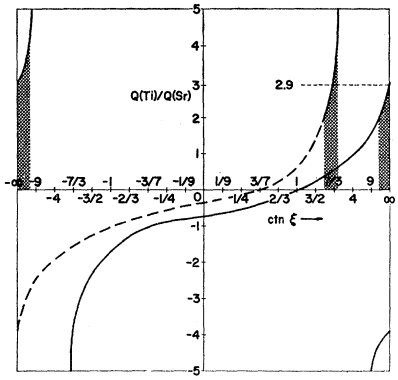

FIG. 2. Apparent charges for $SrTiO_3$ versus ξ. Over much of the range of ξ, the apparent charges of the cations differ widely from the values expected on a dipole local-field model, $Q_{Ti}/Q_{Sr}=2.9$. The shaded fields indicate regions in which $2<(Q_{Ti}/Q_{Sr})\leq 4$ for alternative solutions.

straint ξ.[19] [Actually the indeterminancy in the sign of $\mathcal{P}_{\alpha j}$ results in four physically distinct sets of solutions for $Q(\xi)$.] The preceding study of the local-field approximation suggests the following criteria for physically acceptable sets of effective charges.

(1) $|Q_{Z\parallel}|>|Q_{Z\perp}|$. It is difficult to imagine short-range polarization effects large enough to erase the pronounced anisotropy predicted in Table I.

(2) The ratio of the effective charges of the cations, (Q_B/Q_A), is correctly given by the dipole local-field model. This choice is made as a result of the observation that in this model the effective charges of both cations are relatively insensitive to the parameters describing the local field and are in fact not far from $Q_\kappa=\frac{1}{3}(\epsilon_\infty+2)Z_\kappa$, expected for a diagonally cubic crystal.

(3) In conjunction with (2) above, some assumption must be made concerning Z_B/Z_A. An analysis of the electronic energy bands of $SrTiO_3$ suggest $(Z_{Ti}/Z_{Sr})\approx$ 1.6 to 1.7, but comparable analyses are not available for the remaining materials. In order to give a uniform treatment $(Z_{Ti}/Z_{Ba})=(Z_{Ti}/Z_{Sr})=(Z_{Co}/Z_F)=2.0$ and $(Z_{Ta}/Z_K)=5.0$ is assumed. As Fig. 2 shows specifically for $SrTiO_3$, a variation of as much as a factor of two in (Q_A/Q_B) produces tolerable changes in the predicted values of ξ. Figure 2 also illustrates the fact that a two-fold ambiguity still remains in the eigenvectors $\mathbf{u}(\xi)$, which reflects the uncertainty in the relative directions of the polarizations in the two lowest modes. The apparent charges obtained in this way are given in Table III, and the alternative sets of eigenvectors are presented in Figs. 3 and 4.

TABLE III. Apparent charges of several perovskites derived from optical mode strengths.

	$BaTiO_3$	$SrTiO_3$	$KTaO_3$	$KCoF_3$
A	2.9	2.4	1.2	0.9
B	6.7	7.0	8.1	1.8
$X_{\parallel}$	−4.8	−5.8	−6.3	−2.5
$X_\perp$	−2.4	−1.8	−1.5	−0.1

[19] An equivalent alternative to the introduction of apparent charges through the mode strengths is through the frequencies of the longitudinal modes. For longitudinal modes there is an additional macroscopic electric field given by Eq. (3) (with $\mathbf{E}_0=0$) which causes an additional stiffness so that Eq. (4) becomes $\Omega'_j{}^2\mathbf{m}u'_{\alpha j}=[\mathbf{M}+(4\pi/v)\mathbf{Q}(\epsilon^\infty)^{-1}\mathbf{Q}^+]\mathbf{u}'_{\alpha j}$ for the longitudinal eigenmodes. A procedure which adjusts $Q(\xi)$ using the above equation to obtain the proper longitudinal eigenfrequencies could be adopted but is entirely equivalent to the one used.

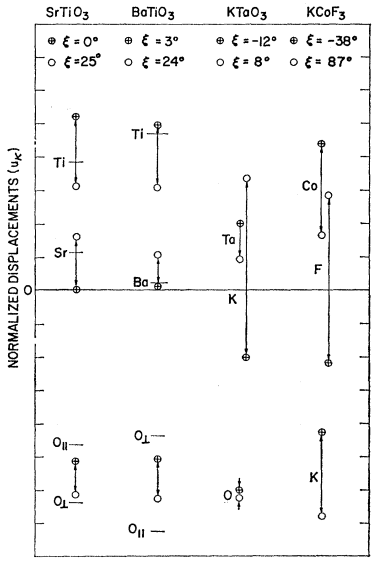

FIG. 3. The eigenvectors of the lowest-frequency polar vibrational modes of several perovskites. The displacements are all normalized to the same (arbitrary) value $\Sigma m_\kappa u_{\kappa j}=N$. Since the alternative solutions are physically not equally likely, the line connecting them is not an "error" bar in any normal sense, but merely aids a comparison of the differences of the two solutions. For $BaTiO_3$, the solid lines are the appropriately normalized spontaneous displacements of the room-temperature tetragonal phase. For $SrTiO_3$ the solid lines are the results of Cowley's shell-model calculation.

V. COMPARISONS AND DISCUSSION

There are several ways in which the results of the preceding section may be examined and further compared with experimental data. The most interesting

TABLE IV. Comparison of calculated and observed room-temperature spontaneous polarization of $BaTiO_3$. The displacements δ_1 are chosen so that the center of mass of the cubic phase is not displaced.

	δ_i[a] (Å)	$P_i=Q_i\delta_i$ μC cm^{-2}	P_i/P_T
Ba	0.003	0.2	0.007
Ti	0.058	9.8	0.360
$O_\parallel$	−0.090	10.7	0.396
$O_\perp$	−0.054	3.2	0.118

$P_{calc}=\Sigma P_i=27.1$ μC cm^{-2}; $P_{obs}=26$ μC cm^{-2}

[a] B. C. Frazer, H. R. Danner, and R. Pepinsky, Phys. Rev. **100**, 745 (1955).
[b] W. J. Merz, Phys. Rev. **91**, 513 (1953).

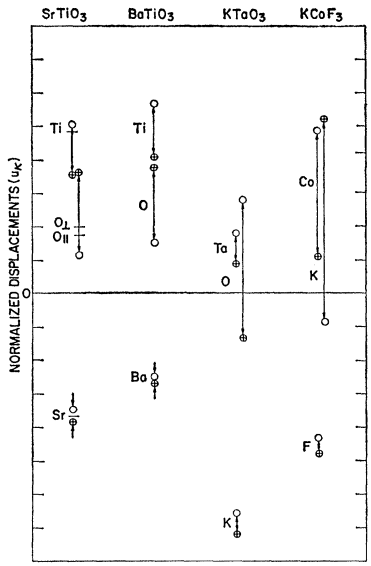

FIG. 4. The eigenvectors of the intermediate-frequency optically active vibrational mode of several perovskites. See legend of Fig. 3 for details. By hypothesis, the eigenvectors of the high-frequency mode consists solely of out-of-phase motion of the $O_{\parallel}$ sublattice against the $O_{\perp}$ sublattices (S_3). As a consequence of this assumption, all oxygen sublattices move together in the two lower-frequency modes.

and important test of the validity of the apparent charges derived here for $BaTiO_3$ is to use them in conjunction with the measured nuclear displacements which occur in passing from the cubic phase to the ferroelectric phases to predict the spontaneous polarization using Eq. (2). For the tetragonal phase the displacements are entirely along a cubic axis, and the calculation is summarized in Table IV. The agreement is sufficiently close that no significance can be attached to the discrepancies.

In the orthorhombic phase, the displacements are such that the net polarization is along a ⟨110⟩ cube direction. The product of the apparent charges times the displacements predicts a spontaneous polarization of 27.7 $\mu C/cm^{-2}$ for this phase as compared with the measured value of 30 $\mu C/cm^{-2}$.

Inspection of Table III shows the pronounced anisotropy in the anion charge anticipated in the local-dipole field treatment to be present although somewhat reduced. (It is the source of polarization in the highest-frequency polar mode.) Furthermore, the two sets of apparent charges can be brought into reasonable agreement only if the static charges Z_i are reduced to about 60% of the formal charges. Reduction of the formal charge of Ti ion in $SrTiO_3$ by roughly this amount due to covalency has been suggested by the band structure calculations of Kahn and Leyendecker[20] and Simanek and Sroubek.[21] The uv optical studies of Cardona[22] are in agreement, as are roughly the Mössbauer isomer shift results of Bhide and Multani.[23] Of course, the ions in the A site are expected to be less affected by covalency.

Turning now to a consideration of the normal modes, those given by Cowley[5] for $SrTiO_3$ must be considered as the most reliable presently available. It is readily apparent from Figs. 3 and 4 that either of the alternative sets developed here primarily from infrared polarization data are recognizably related to those obtained from the more detailed neutron-scattering results. Of the two, the $\xi=25°$ solution agrees nearly twice as well as the $\xi=0°$ solution.

In the case of $BaTiO_3$, Fig. 3 shows a comparison of the predicted eigenvectors for the soft mode in the cubic phase and the relative spontaneous displacements which the ions undergo when passing from the cubic to the tetragonal phase. Kwok and Miller[24] have recently provided a theoretical foundation for the often expressed suggestion that these two sets of displacements are proportional. Once again from the comparison in Fig. 3, either mode set is recognizably close to the measured displacements, the rms differences (8% or 14%) being probably within the uncertainty in the observations themselves.

Because of the intimate connection of the ferroelectric phenomena with lattice modes in $BaTiO_3$ the description of these modes has been much discussed. By comparing the infrared spectra of $SrTiO_3$ and $BaTiO_3$ with that of TiO_2, Spitzer *et al.*,[4] concluded that the intermediate-frequency mode could be interpreted as a (cation)-(TiO_3) vibration (i.e., closely similar to the symmetry mode S_2). Last[6] had originally suggested that this (cation)-(TiO_3) mode should be attributed to the lowest-frequency mode. Perry, Khanna, and Rupprecht[25] favored Last's assignment because in a comparative study of several titanium perovskites the frequency of the lowest mode was by far the most sensitive to changes in the type A cation. In their treatment of $SrTiO_3$, Joseph and Silverman[19] were unable to distinguish between a set of solutions for the soft mode corresponding more or less to Last's original description, and another set similar to symmetry coordinate S_1, which they termed a "Slater"-type solution because it implied a weakening of the $Ti-O_{\parallel}$ coupling anticipated by Slater.[8] Obviously the form of (particularly the low-frequency) modes is a matter of some dispute in the current literature despite (or perhaps because of) the amount of work bearing on the subject. For the oxides considered here, the present results seem quite clear cut (as is nicely shown in Fig. 2 for $SrTiO_3$). *Reasonable assignments of apparent charges can only be made when the lowest-frequency mode is recognizably close to a "Slater" mode (symmetry*

[20] A. H. Kahn and A. J. Leyendecker, Phys. Rev. **135**, A1321 (1964).
[21] E. Simanek and Z. Sroubek, Phys. Status Solidi **8**, K47 (1965).
[22] M. Cardona, Phys. Rev. **140**, A651 (1965).
[23] V. G. Bhide and M. S. Multani, Phys. Rev. **139**, A1983 (1965).
[24] P. C. Kwok and P. B. Miller, Phys. Rev. **151**, 387 (1966).
[25] C. H. Perry, B. N. Khanna, G. Rupprecht, Phys. Rev. **135**, A408 (1964).

coordinate S_1). The modes of intermediate frequency are therefore correspondingly closely related to S_2, as Spitzer *et al.*, have suggested.

On the other hand, the mode pattern for the fluoride seems qualitatively different. Although the difference between the alternative solutions is greater here, at least one of the solutions for the low-frequency mode is very similar to S_2 as Last originally proposed for the oxides, and as would be expected if the negative ions were strongly coupled to the B sublattice and very loosely coupled to the A sublattice. One is tempted to argue that this is indeed the normal state of affairs in a perovskite lattice with anions less polarizable than oxygen and thus unable to supply the favorable long-range $B-X_{||}$ coupling necessary to stabilize the "Slater" mode.

Since the eigenvalues of the dynamical matrix are known experimentally, once the eigenvectors are fixed, the machinery of matrix diagonalization can be reversed to obtain the various sublattice coupling constants. Because of the two-fold ambiguity arising from the eigenvector choice, only general features characteristic of all of the solutions studied are worthy of comment. First of all, the strongest sublattice coupling in all cases is between the anions. This is of course a direct consequence of the assumption concerning the form of the high-frequency modes, but an argument for its physical plausibility has been made as well. The second feature common to all solutions is the small magnitude of the net $B-X$ coupling constants. In fact for $BaTiO_3$, $SrTiO_3$, and one of the two $KTaO_3$ solutions, the coupling constants are found to be attractive (i.e., a displacement of X toward B results in a force on B directed towards X). It is of course obvious that this situation favors the ferroelectric transition. This situation can be understood to come about in large measure from the abnormal long-range force constants calculated in Sec. II, which in turn have their origin in the high-local electric fields existing along the $B-X_{||}$ axis, just as Slater visualized.

PHYSICAL REVIEW VOLUME 157, NUMBER 2 10 MAY 1967

Infrared Dielectric Dispersion of Several Fluoride Perovskites

J. D. Axe* and G. D. Pettit
IBM Watson Research Center, Yorktown Heights, New York

(Received 2 December 1966)

Measurements at room temperature of the infrared reflectivity, low-frequency dielectric constant (ϵ_0), and optical index of refraction (n) have been made on $KCoF_3$, $KMnF_3$, and $RbMnF_3$. The reflectivity data have been analyzed using Kramers-Kronig relations to obtain the dielectric dispersion from 50 cm^{-1} to 4000 cm^{-1}. The frequencies of the three transverse optic (longitudinal optic) long-wavelength polar eigenmodes are 139 (168), 225 (293), 417 (500) cm^{-1} for $KCoF_3$; 115 (143), 193 (268), 395 (479) cm^{-1} for $KMnF_3$ and 113 (124), 197 (273), 369 (452) cm^{-1} for $RbMnF_3$. $\epsilon_0=7.35$, 8.28, 7.6 and $n=1.47$, 1.44, 1.53 for $KCoF_3$, $KMnF_3$, and $RbMnF_3$, respectively. Mode strengths and damping were also measured. Low-temperature reflectivity measurements on antiferromagnetically ordered $KCoF_3$ were also performed.

I. INTRODUCTION

THE study of the lattice dynamics of the cubic perovskite structure has proved quite fruitful. Many, though by no means all, of the binary oxide perovskites are unstable and distort spontaneously at low temperatures into ferroelectrically or antiferroelectrically ordered states.[1] In their cubic phases these compounds have large low-frequency dielectric constants which arise predominantly from the response of the lowest frequency polar eigenmode of long wavelength.[2–5] Compounds other than binary oxides having the perovskite structure seem not to have anomalous dielectric properties, and it is interesting to inquire into the underlying causes for these differences. The alkali-transition metal fluorides are well suited for such a study. An additional incentive for studying these compounds is that they are known to undergo structural changes accompanying magnetic ordering which must also ultimately be understood on the basis of lattice dynamical considerations.

II. RESULTS

Samples were cut and polished by standard metallographic procedures, with a final polish on 0.05-μ alumina. All reflectivities were measured at room temperature and near normal incidence using point by point comparison with an aluminized surface in a Perkin-Elmer model 301 spectrometer.[6] The frequency

* Partially supported by Army Research Office, Durham, North Carolina, under Contract No. DA-31-124-ARO-D-205.

[1] For a review of the dielectric properties of perovskite-type ferroelectrics see F. P. Jona and G. Shirane, *Ferroelectric Crystals* (Pergamon Press, Inc., New York, 1962), Chap. V.

[2] W. Cochran, Advan. Phys. **9**, 387 (1960).

[3] A. S. Barker and M. Tinkham, Phys. Rev. **125**, 1527 (1962).

[4] W. G. Spitzer, R. C. Miller, D. A. Kleinman, and L. E. Howarth, Phys. Rev. **126**, 1710 (1962).

[5] R. A. Cowley, Phys. Rev. **134**, A981 (1964).

[6] See J. D. Axe, J. W. Gaglianello, and J. E. Scardefield, Phys. Rev. **139**, A1211 (1965) for additional experimental details. In the present work, no attempt was made to check for surface damage. It was shown to be negligible in previous fluorides studied.